Available online at www.sciencedirect.com
ScienceDirect
Ceramics International 36 (2010) 929–935
CERAMICS INTERNATIONAL
www.elsevier.com/locate/ceramint

Moisture sensitivity of $YCr_{(1-x)}Mn_xO_3$ perovskites

Christelle Nivot, Jérôme Bernard *, C. Lelievre, Jean-Marie Haussonne, David Houivet

LUSAC (EA4253), Site Universitaire, B.P. 78, 50130 Cherbourg Octeville, France

Received 14 September 2009; received in revised form 6 October 2009; accepted 20 October 2009
Available online 20 November 2009

Abstract

This work deals with the sensitivity to moisture rate in air of perovskite with general formula $YCr_{(1-x)}Mn_xO_3$ with x ranging from 0 to 0.8. The combined sensitivity to moisture and temperature let us think the possibility of realizing composite sensors temperature/moisture. This study clearly shows the influence of the Mn content on moisture which affects the working frequency of sensors. Capacitance variation of the most sensitive compositions increases from 100 pF to 1 nF for relative humidity between 20 and 80%. The influence of porosity is also demonstrated.

Keywords: C. Dielectric properties; D. Perovskite; E. Thermistors; E. Sensors

1. Introduction

A great attention [1,2] is paid to monitoring and controlling moisture in various domains like automobile, agriculture, industry or domestic comfort. Materials used in humidity sensors are mainly electrolytes, organic polymers and ceramics. These materials are used for their sensitivity to the air moisture. Large sensitivity over the entire range of moisture, low hysteresis, short response time, long durability and stability of properties with time are required. However, each of the sensors previously listed has limitations. Indeed, humidity sensors show slow response time [3] and polymer films present degradations upon exposure to some solvents [4]. Despite their chemical, physical and thermal stabilities, porous ceramic sensors present disadvantage of pollution matter because of impurities adsorption at the surface.

Ceramics types sensors have been studied as porous traditionally sintered bodies [5,6] and thick [7–9] or thin [10–12] films. The principle of humidity measurement is based on the change of electrical properties such as resistance and capacitance versus relative humidity. Different types of conduction are at the origin of the humidity sensitivity [13]: ionic, electronic and solid electrolytes. Whatever the conduction type is, humidity sensitivity is due to the formation of chemically adsorbed layer of OH^- ions bonded to metal ions at the oxide surface. In the case of ionic conduction, hopping of proton H^+, resulting from water dissociation in the physisorbed layer, from one adsorbed H_2O molecule to another (Grotthus chain reaction) causes charge transport in the layers of physically adsorbed water. At high humidity level, liquid water condenses in the pores and electrolytic conduction takes place in addition to the H^+ transport in adsorbed layers. Electronic conduction takes place between chemisorbed water molecules and semiconducting ceramic materials including perovskite-type and spinel-type [14] oxides.

For perovskites, the doping of $BaTiO_3$ with a certain amount of impurities leads to an increase of sensitivity to moisture rate in air and a decrease of hysteresis [15]. It is established [12] that barium perovskites used as thin films show humidity sensitivity, fast response, negligible hysteresis and good long-term stability. Moreover, the response of porous ceramics with composition $BaMO_3$ (with M = Ti, Zr, Hf or Sn) showed a sensitivity of capacitance with humidity.

A previous work [16], concerning perovskite-type oxides, showed good properties as NTC resistors which are two-phased compounds belonging to the system aY_2O_3–$bYCr_{0.5}Mn_{0.5}O_3$. The aim of this work is the study of such perovskite used as humidity sensor. Humidity sensitive characteristics as capacitance and resistance are investigated. Existence of hysteresis on these characteristics is tested. In a first part, we studied the humidity effect on electrical properties of $YCr_xMn_{1-x}O_3$. In a second part, we studied the influence of a certain amount of Y_2O_3 addition on $YCr_xMn_{1-x}O_3$ response.

* Corresponding author. Tel.: +33 233014233; fax: +33 233014135.
E-mail address: jerome.bernard@unicaen.fr (J. Bernard).

0272-8842/$36.00
doi:10.1016/j.ceramint.2009.10.021

Fig. 1. Layout of the sensor.

2. Experimental

aY_2O_3–$bYCr_xMn_{1-x}O_3$ compounds were prepared by solid-state reaction, with a included between 0 and 0.8 and $x = 0.25$, 0.5 and 0.75. Y_2O_3 (Aldrich 99.99%), Cr_2O_3 (Riedel-deHaën 99%) and Mn_2O_3 (Riedel-deHaën 99%). Powders were mixed into an aqueous slurry. After drying, the powders were calcined at 1200 °C, disagglomerated and pressed at 175 MPa into 20 mm diameter and about 3 mm high pellets. Samples were sintered at 1600 °C for 5 h. A comb type Au (Fig. 1) was deposited on sintered samples and then components were heated at 850 °C.

Relative densities of samples were obtained with helium pycnometer (Micromeritics AccuPyc 1330). The electrical response to humidity of samples was investigated by capacitance measurements and dc resistance measurements at 25 °C. Characterisations were carried out into a Secasi SLH100/70® climate chamber. Capacitance measurements were performed with a RCL meter Fluke PM6306® and dc resistance measurements with a Sefelec M1500P megohm-meter.

3. Results and discussion

3.1. $YCr_xMn_{1-x}O_3$ ceramics

3.1.1. Structural characterisations

XRD patterns performed on sintered pellets revealed the existence of two phases depending of x value as shown in Fig. 2. For $x = 0.25$, two phases are present: $YMnO_3$ and $YCrO_3$. For $x = 0.5$ and $x = 0.75$, only the orthorhombic perovskite phase isomorphic to $YCrO_3$ is present. However, the peaks are shifted compared to the theoretical ones. That is the consequence of substitution of Mn^{3+} for Cr^{3+} in the $YCrO_3$ perovskite lattice. Moreover, for $x = 1$, peaks corresponding to Y_2O_3 and Cr_2O_3 are detected which is due to an incomplete reactive calcination.

3.1.2. Frequency sensitivity

The capacitance of the sensor depends on the measurements frequency. Humidity response was measured in the range of 100 Hz to 1 kHz for different relative humidities as represented in Fig. 3. The most sensitive response of capacitance is obtained for a frequency of 100 Hz. Therefore, all measurements are performed at 100 Hz and 25 °C.

3.1.3. Humidity response of $YCr_xMn_{1-x}O_3$ sensors

The resistance of $YCr_xMn_{1-x}O_3$ materials with $x = 0.5$ and 0.25 is constant and relatively weak whatever the relative humidity (Fig. 4). Material with composition $YCr_{0.75}Mn_{0.25}O_3$ has a resistance which slightly decreases when relative humidity increases. The most sensitive and the higher resistance material is the one with composition $YCrO_3$. The dc resistance of this material decreases by one order of magnitude over the measured range of relative humidity. Another observation concerns Cr ratio influence on resistance

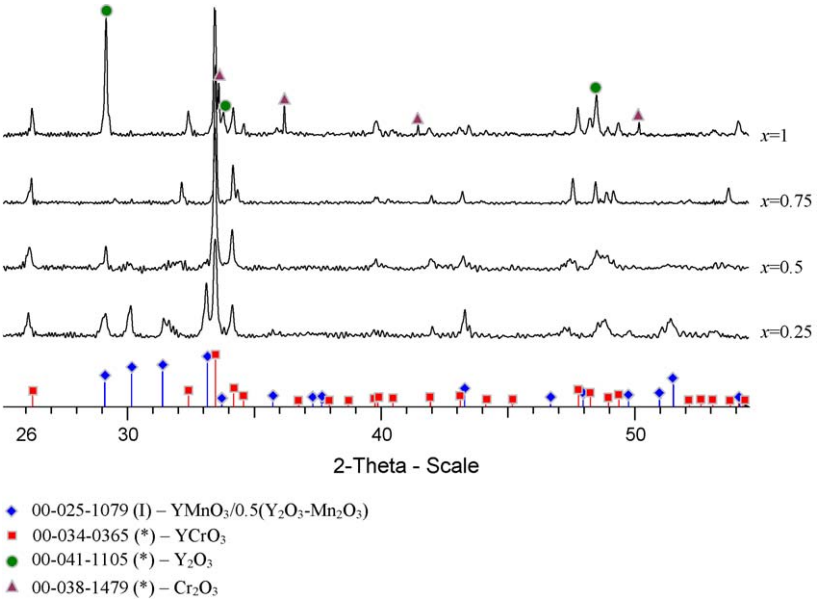

Fig. 2. XRD patterns of compositions $YCr_xMn_{1-x}O_3$ sintered at 1600 °C.

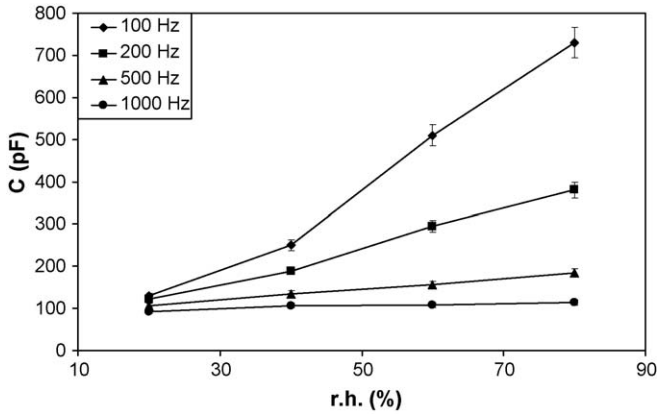

Fig. 3. Capacitance response as a function relative humidity for different frequencies between 100 and 1000 Hz.

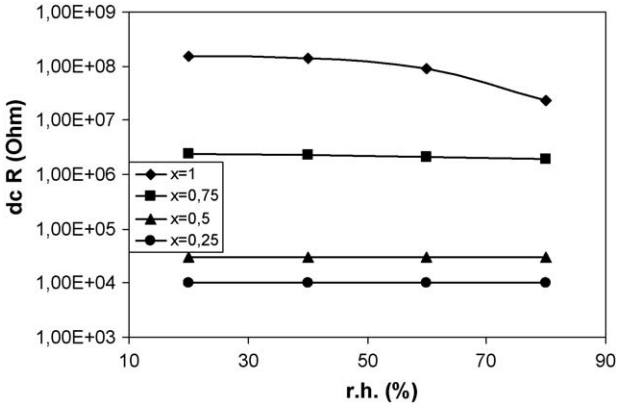

Fig. 4. dc resistance evolution of $YCr_xMn_{1-x}O_3$ materials as a function of relative humidity.

versus relative humidity. When x increases, sensitivity and resistance value increase whatever the relative humidity is.

Fig. 5 shows a capacitance sensitivity which depends on the tested material composition. Indeed, $YCrO_3$ samples present poor sensitivity whereas $YCr_{0.25}Mn_{0.75}O_3$ materials have capacitance which is quite sensitive from 20% r.h. to 80% r.h. $YCr_{0.75}Mn_{0.25}O_3$ and $YCr_{0.5}Mn_{0.5}O_3$ samples present

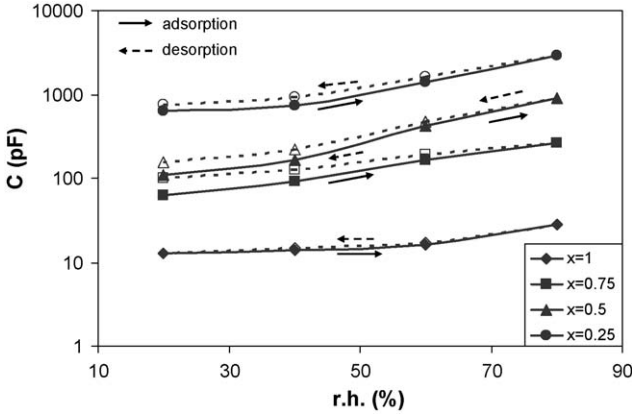

Fig. 5. Capacitance evolution of $YCr_xMn_{1-x}O_3$ materials as a function of relative humidity.

Table 1
Relative density of sintered materials $YCr_xMn_{1-x}O_3$.

x	1	0.75	0.5	0.25
Relative density	$0.51 \pm 0.02\%$	$0.60 \pm 0.01\%$	$0.70 \pm 0.02\%$	$0.86 \pm 0.03\%$

intermediate behaviour with a quite good sensitivity. Whatever the tested materials compositions are, capacitance increase with relative humidity is attributed to the effect of multilayers of physically adsorbed water [12].

In order to observe saturation on $YCr_xMn_{1-x}O_3$ humidity sensitive materials, capacitance evolution was measured during the hysteresis cycle (adsorption–desorption) in the range of [80%; 20%]. Results represented in Fig. 2 (dot lines) highlight water saturation of materials with compositions: $YCr_{0.75}Mn_{0.25}O_3$, $YCr_{0.5}Mn_{0.5}O_3$ and $YCr_{0.25}Mn_{0.75}O_3$ since initial results are not reached after an exposure to high moisture degree. Moreover, it must be noted that the more is the saturation the more is x value high. Saturation is not observable on $YCrO_3$ but this is due to the initial low value of the capacitance and measurement is within the detection limit of RCL meter used for characterizations.

The densification degree of the materials is an important factor which determines their humidity sensitivity. Table 1 summarizes relative density results obtained on materials by He pycnometry.

Comparison of results obtained by helium pycnometry with those on saturation show a correlation between the densification degree of materials and their sensitivity to saturation. The less a sample is densified the more it tends to be saturated.

The second part of this work was aimed at improving the densification of materials in order to reduce saturation after long exposure under high moisture exposition.

3.2. aY_2O_3–$bYCr_xMn_{1-x}O_3$ ceramics

Previous work [16] showed that the addition of Y_2O_3 to a $YCrO_3$ derived phase presents two advantages, i.e. a densification improvement and an increasing of resistance. On the other hand, Fig. 5 showed a too weak capacitance evolution of the $YCrO_3$ composition in the range of relative humidities tested. So, in the light of these results, aY_2O_3–$bYCr_xMn_{1-x}O_3$ compositions with $x = 0.25$, 0.5 and 0.75 were elaborated and their electric properties were measured.

3.2.1. Structural characterisation

For $x = 0.75$ and $x = 0.5$, Fig. 6(a) and (b) indicates materials to be two-phased ceramics whatever the b value. Indeed, Y_2O_3 and orthorhombic perovskite phase isomorphic to $YCrO_3$ were detected in different proportions according to b value. For compositions with $x = 0.25$, XRD analyses shows the presence of three phases: $YCrO_3$, $YMnO_3$ and Y_2O_3. For decreasing b value, the presence of Y_2O_3 is to be noted.

3.2.2. Humidity response of aY_2O_3–$bYCr_xMn_{1-x}O_3$ sensors

For each x value, the addition of Y_2O_3 to the $YCr_xMn_{1-x}O_3$ phase implies a dc resistance increase as expected (Fig. 7).

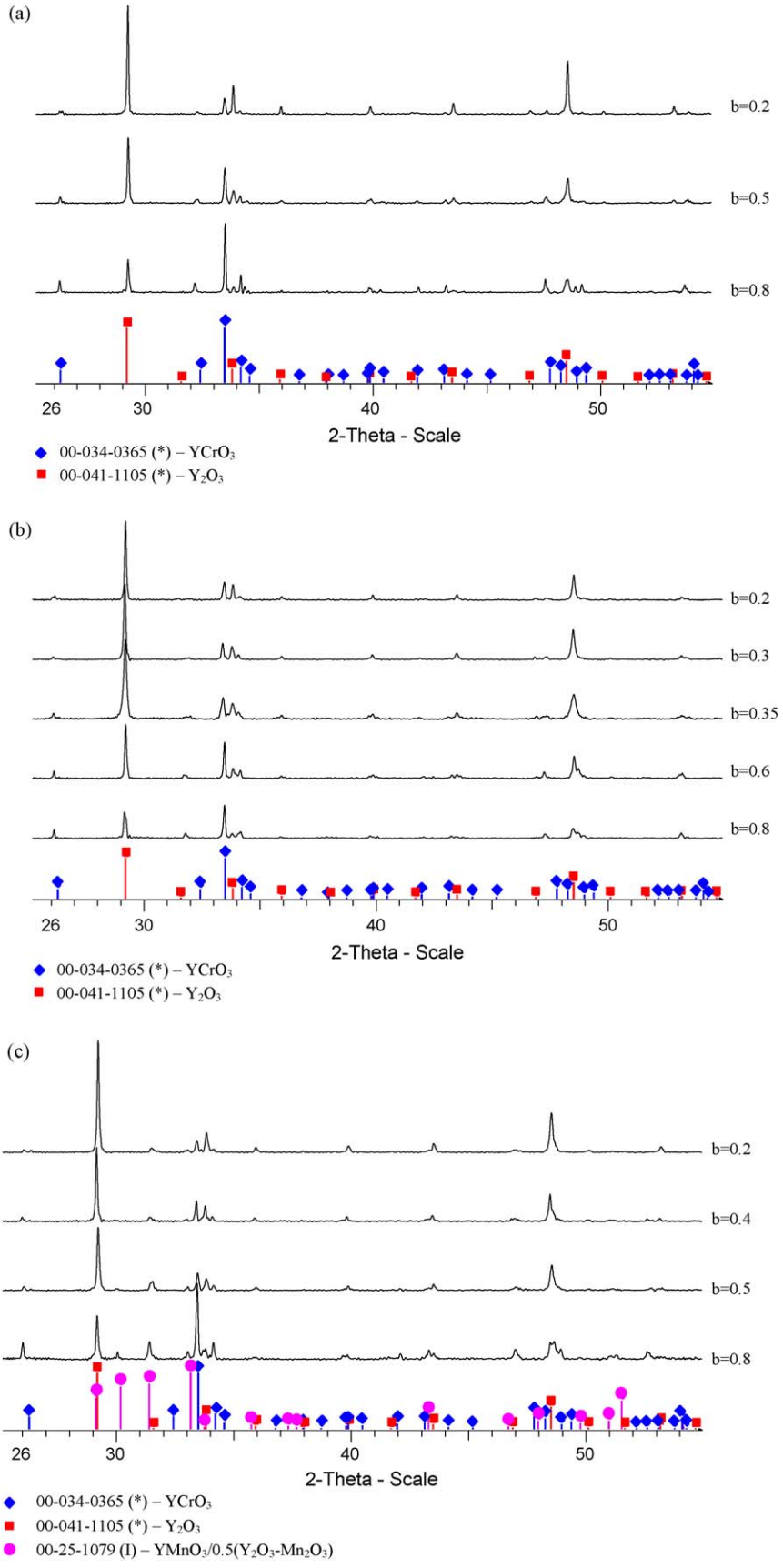

Fig. 6. XRD patterns of compositions aY_2O_3–$bYCr_xMn_{1-x}O_3$ with (a) $x = 0.75$, (b) $x = 0.5$ and (c) $x = 0.25$.

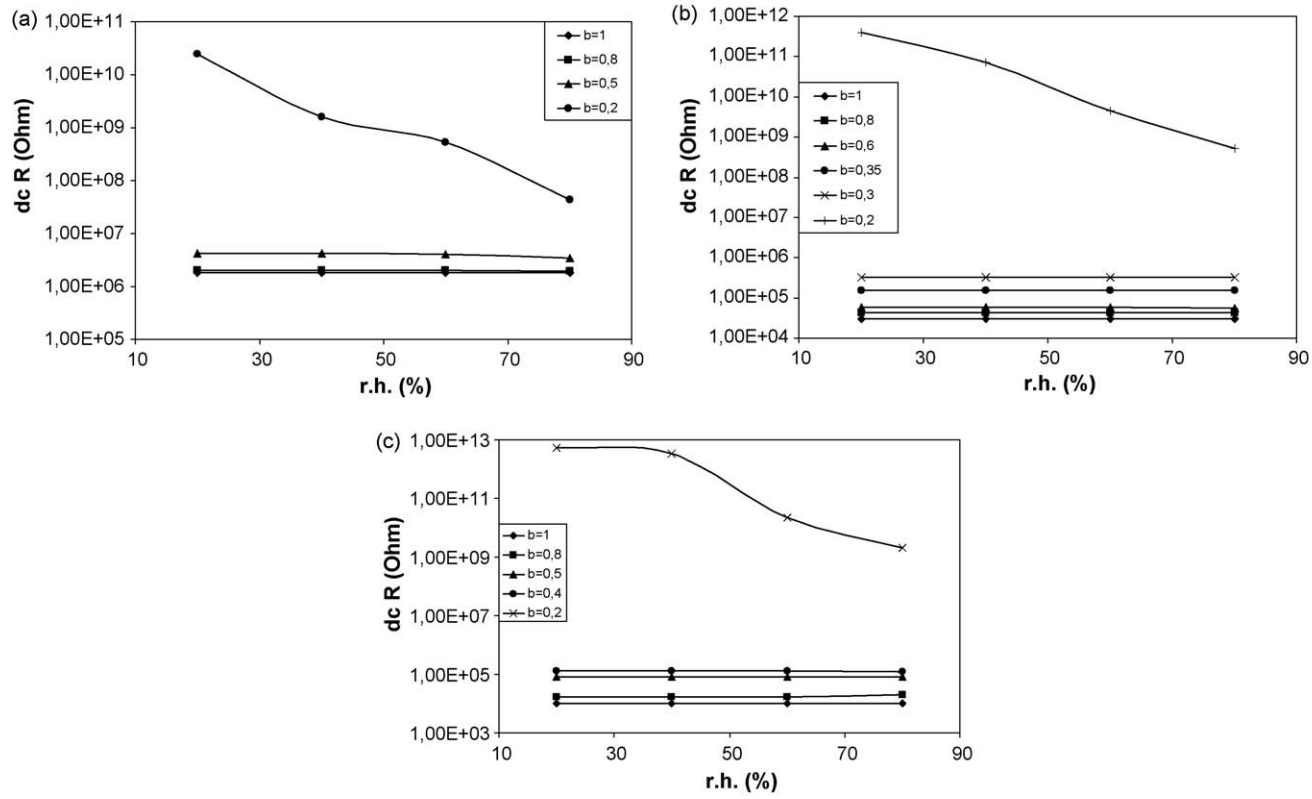

Fig. 7. dc resistance evolution as a function of the relative humidity of compositions aY_2O_3–$bYCr_xMn_{1-x}O_3$ for (a) $x = 0.75$, (b) $x = 0.5$ and (c) $x = 0.25$.

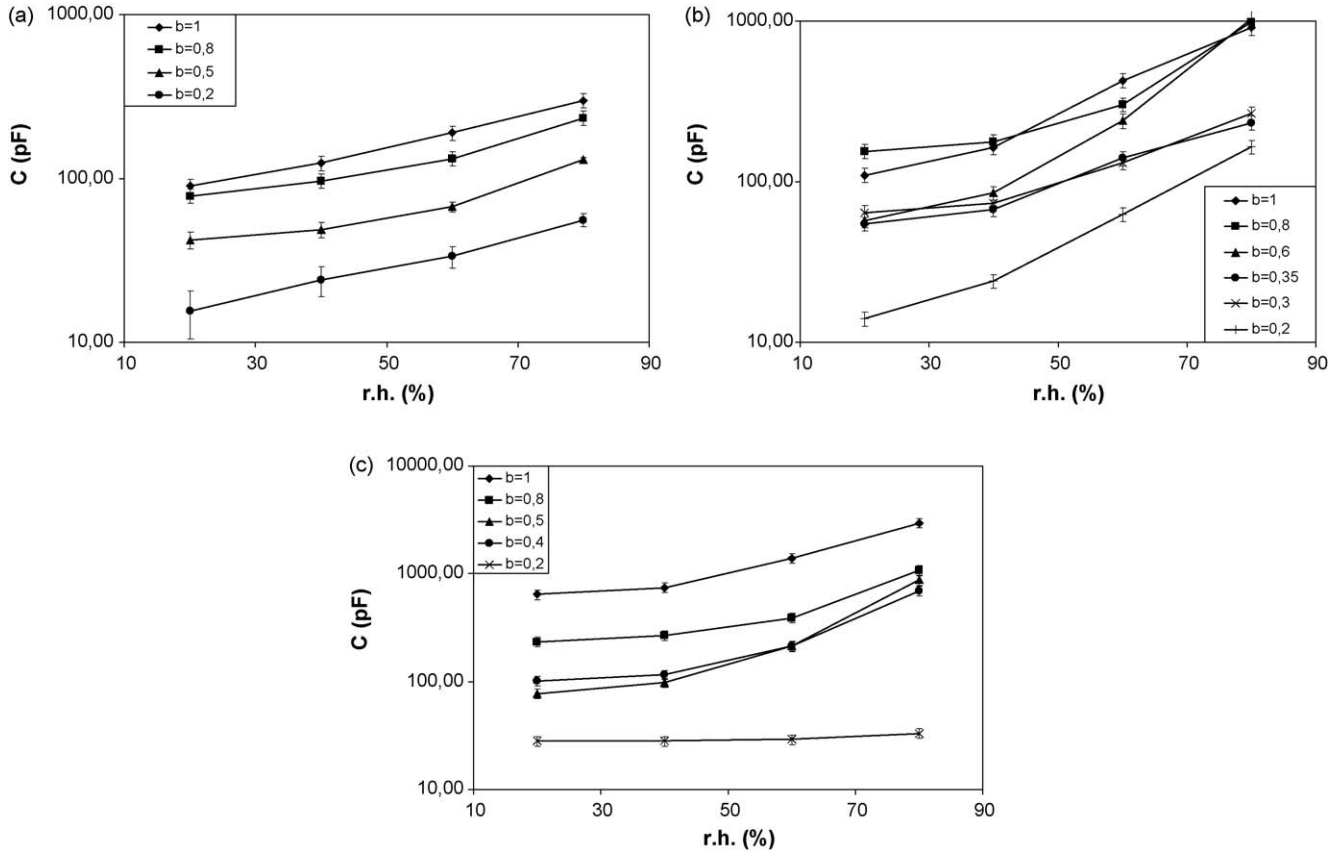

Fig. 8. Capacitance evolution as a function of the relative humidity of compositions aY_2O_3–$bYCr_xMn_{1-x}O_3$ for (a) $x = 0.75$, (b) $x = 0.5$ and (c) $x = 0.25$.

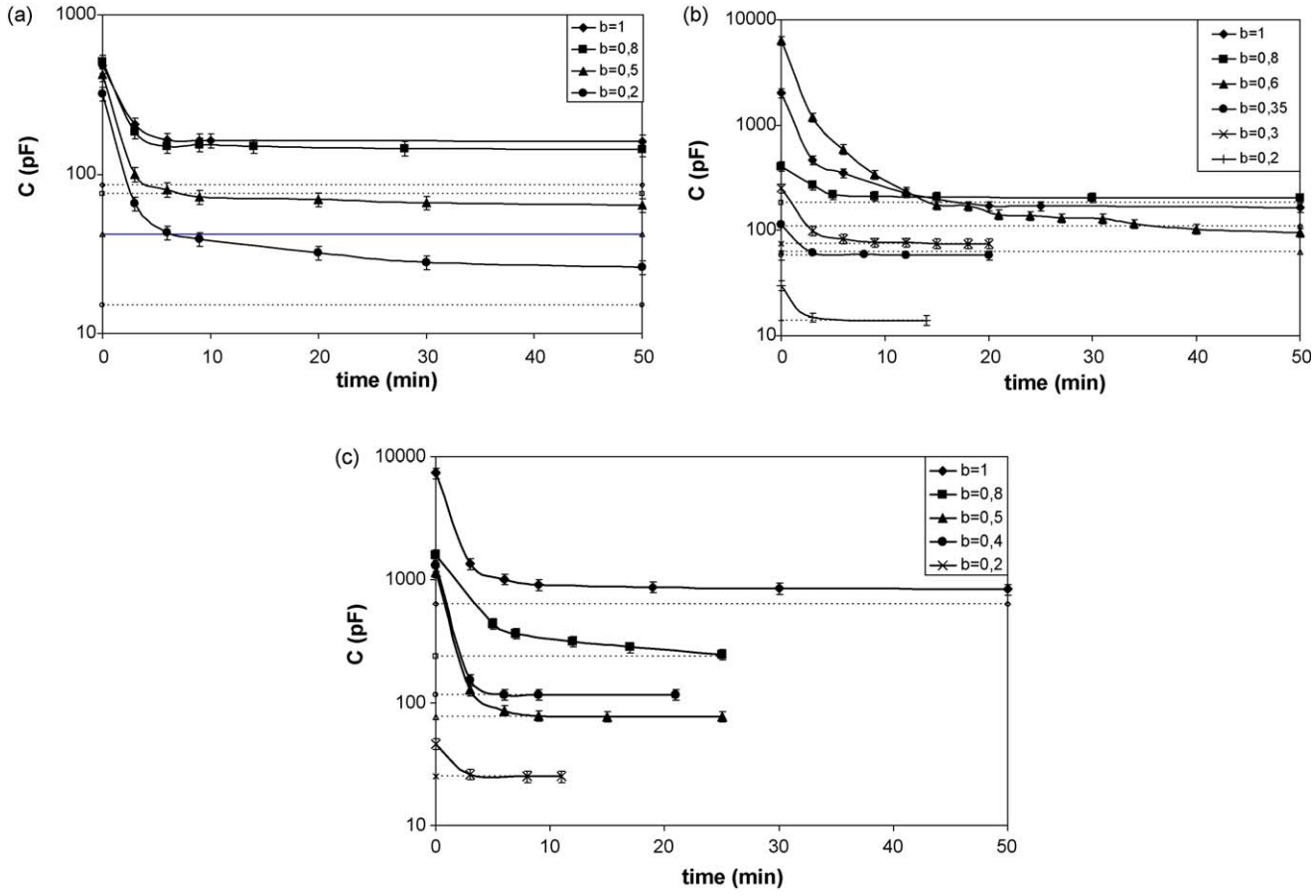

Fig. 9. Time to return at initial capacitance value (r.h. = 20%) after long exposure at r.h. > 90% for aY_2O_3–$bYCr_xMn_{1-x}O_3$ compositions with (a) $x = 0.75$, (b) $x = 0.5$ and (c) $x = 0.25$.

Moreover, when a weak amount of Y_2O_3 is added, the resistance remains constant almost 1 MΩ and insensitive to environmental moisture. On the other hand, for $0.8Y_2O_3$–$0.2YCr_xMn_{1-x}O_3$ compositions, an increase of resistance for 20% r.h. These materials present a resistance which is highly sensitive to relative humidity since dc resistance value decreases by several orders of magnitude over the measured range.

Compared with results obtained on $YCr_xMn_{1-x}O_3$ compositions, capacitance sensitivity is globally maintained when Y_2O_3 resistive phase is added as represented in Fig. 8. For a given relative humidity, the capacitance decreases with Y_2O_3 addition. For each elaborated composition, capacitance increases with an increasing relative humidity. On the one hand, the capacitance sensibility of aY_2O_3–$bYCr_{0.75}Mn_{0.25}O_3$ compositions is nearly exponential in all the range of relative humidity whatever the b value. On the other hand, the sensitivity of aY_2O_3–$bYCr_{0.5}Mn_{0.5}O_3$ and aY_2O_3–$bYCr_{0.25}Mn_{0.75}O_3$ compositions for $b \geq 0.4$ at weak relative humidity is lower than at r.h. > 40%. It must be noted that $0.8Y_2O_3$–$0.2YCr_{0.5}Mn_{0.5}O_3$ composition remains sensitive on the range of humidity and $0.8Y_2O_3$–$0.2YCr_{0.25}Mn_{0.75}O_3$ composition has constant capacitance whatever the environmental humidity.

In order to study saturation of aY_2O_3–$bYCr_xMn_{1-x}O_3$ compositions ($x = 0.75$, 0.5 and 0.25), time to return at initial capacitance value (r.h. = 20%) after long exposure at r.h. > 90% was measured (Fig. 9).

In Fig. 9, dotted lines represent initial capacitance value measured at 20% of r.h. Fig. 9(a) illustrates saturation of aY_2O_3–$bYCr_{0.75}Mn_{0.25}O_3$. Whatever b value is, each sample is not able to reach the initial capacitance value even after an exposure of 50 min at 25 °C and 20% relative humidity. For aY_2O_3–$bYCr_{0.5}Mn_{0.5}O_3$ formulations water saturation exists, except compositions with $b \leq 0.35$. Capacitance values are higher than those measured before long exposition at 90%. For aY_2O_3–$bYCr_{0.25}Mn_{0.75}O_3$ compositions, saturation is only observable for material without Y_2O_3 addition ($b = 1$). Indeed $0.2Y_2O_3$–$0.8YCr_{0.25}Mn_{0.75}O_3$ composition presents a light saturation while compositions with $b \leq 0.5$ are not sensitive to the saturation (initial capacitance values are reached after 3 min). It must be noted that 3 min are necessary for the climate chamber to regulate.

These observations are linked to the densification state of the samples. Fig. 10 shows that Y_2O_3 addition significantly increases final density. Thus, comparison with results represented in Fig. 9 indicates that compositions which do not present water saturation are materials with relative density higher than 0.9.

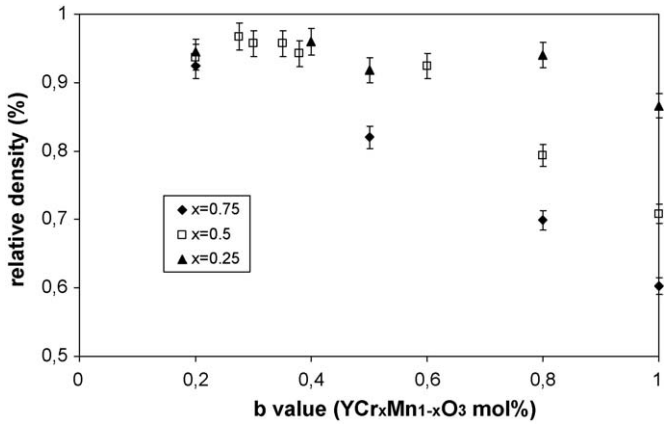

Fig. 10. Densification of aY_2O_3–$bYCr_xMn_{1-x}O_3$ compositions as a function of b ($YCr_xMn_{1-x}O_3$ mol.%).

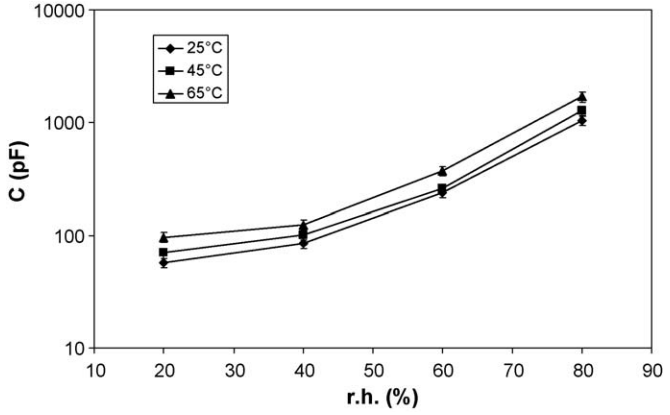

Fig. 11. Capacitance of $0.4Y_2O_3$–$0.6YCr_{0.5}Mn_{0.5}O_3$ composition as a function of relative humidity at 25, 45 and 65 °C.

3.2.3. Temperature dependence

As reported in a previous work [16], aY_2O_3–$bYCr_xMn_{1-x}O_3$ compositions are NTC ceramic resistors. It implies a resistance evolution with temperature and thus a capacitance change too. The capacitances of such compositions are measured as a function of relative humidity for different temperatures: 25, 45 and 65 °C (Fig. 11). Whatever the temperature is, capacitance presents the same increasing behaviour with an increasing relative humidity. For a given relative humidity, capacitance increases with temperature. Therefore, for the use of such compositions as humidity sensors, the temperature compensation is necessary for sharp measurements.

4. Conclusions

$YCr_xMn_{1-x}O_3$ compositions with x between 0.25 and 1 showed a weak sensibility of capacitance and almost no resistance variation in the range of relative humidity. On the other hand, the disadvantage of these compositions is their moisture saturation. This phenomenon is linked to the densification state. Therefore, in order to improve densification a resistive phase: Y_2O_3 is added to the perovskite phase $YCr_xMn_{1-x}O_3$. Humidity response of aY_2O_3–$bYCr_xMn_{1-x}O_3$ compositions showed that this type of material can be used for its sensitivity in the range of the studied relative humidity. Indeed, capacitance of the most sensitive compositions increases from 100 pF to 1 nF for relative humidity between 20 and 80%. For the use of such compositions as humidity sensors, water saturation must be considered since it influences sensor response. Therefore, the most interesting compositions are: $0.8Y_2O_3$–$0.2YCr_{0.5}Mn_{0.5}O_3$ (despite the weak capacitance value for 20% relative humidity) and aY_2O_3–$bYCr_{0.25}Mn_{0.75}O_3$ with b between 0.4 and 0.8 (despite the weak sensitivity of the capacitance for r.h. lower than 40%). An other point which must be considered for the use of such compositions as humidity sensors is the temperature dependence because it influences capacitance results.

References

[1] B.M. Kulwicki, Humidity sensors, J. Am. Ceram. Soc. 74 (4) (1991) 697–708.
[2] E. Traversa, Ceramic sensors for humidity detection: the state-of-the-art and future developments, Sens. Actuators B 23 (1995) 135–156.
[3] P. Shuk, M. Greenblatt, Solid electrolyte film humidity sensor, Solid State Ionics (1998) 113–115, 229–233.
[4] B. Adhikari, S. Majumdar, Polymers in sensor applications, Prog. Polym. Sci. 29 (2004) 699–766.
[5] T.J. Hwang, G.M. Choi, Humidity response characteristics of barium titanate, J. Am. Ceram. Soc. 76 (3) (1993) 766–768.
[6] M. Viviani, M.T. Buscaglia, V. Buscaglia, M. Leoni, P. Nanni, Barium perovskites as humidity sensing materials, J. Eur. Ceram. Soc. 21 (2001) 1981–1984.
[7] J. Holc, J. Slunecko, M. Hrovat, Temperature characteristics of electrical properties of (Ba, Sr)TiO_3 thick film humidity sensors, Sens. Actuators B 26–27 (1995) 99–102.
[8] W. Qu, J.-U. Meyer, A novel thick-film ceramic humidity sensor, Sens. Actuators B 40 (1997) 175–182.
[9] J. Huang, Y. Hao, H. Lin, D. Zhang, J. Song, D. Zhou, Preparation and characteristic of the thermistor materials in the thick-film integrated temperature-humidity sensor, Mater. Sci. Eng. B 99 (1–3) (2003) 523–526.
[10] W. Qu, W. Wlodarski, A thin-film sensing element for ozone, humidity and temperature, Sens. Actuators B 64 (2000) 42–48.
[11] W. Qu, W. Wlodarski, J.-U. Meyer, Comparative study on micromorphology and humidity sensitive properties of thin-film and thick-film humidity sensors based on semiconducting $MnWO_4$, Sens. Actuators B 64 (2000) 76–82.
[12] J. Yuk, T. Troczynski, Sol–gel $BaTiO_3$ thin film for humidity sensors, Sens. Actuators B 94 (2003) 290–293.
[13] J.G. Fagan, V.R.W. Amarakoon, Reliability and reproducibility of ceramic sensors. Part III. Humidity sensors, Am. Ceram. Soc. Bull. 72 (3) (1993) 119–130.
[14] S.S. Pingale, S.F. Patil, M.P. Vinod, G. Pathak, K. Vijayamohanan, Mechanism of humidity sensing of Ti-doped $MgCr_2O_4$ ceramics, Mater. Chem. Phys. 46 (1996) 72–76.
[15] J. Wang, B. Xu, G. Liu, J. Zhang, T. Zhang, Improvement of nanocrystalline $BaTiO_3$ humidity sensing properties, Sens. Actuators B 66 (2000) 159–160.
[16] D. Houivet, J. Bernard, J.-M. Haussonne, High temperature NTC ceramic resistors (ambient-1000 °C), J. Eur. Ceram. Soc. 24 (2004) 1237–1241.